IEEE Access
Multidisciplinary | Rapid Review | Open Access Journal

Received June 5, 2018, accepted July 8, 2018, date of current version September 5, 2018.

Digital Object Identifier 10.1109/ACCESS.2018.2859434

Microwave Imaging for Breast Tumor Detection Using Uniplanar AMC Based CPW-Fed Microstrip Antenna

MD. ZULFIKER MAHMUD[1,2], (Student Member, IEEE), MOHAMMAD TARIQUL ISLAM[2], (Senior Member, IEEE), NORBAHIAH MISRAN[2], (Member, IEEE), SALEHIN KIBRIA[2], AND MD. SAMSUZZAMAN[2], (Student Member, IEEE)

[1]Department of AIS, Jagannath University, Dhaka 1100, Bangladesh
[2]Centre of Advanced Electronic and Communication Engineering, Faculty of Engineering and Built Environment, Universiti Kebangsaan Malaysia, Bangi 43600, Malaysia

Corresponding authors: Md. Zulfiker Mahmud (zulfikerm@siswa.ukm.edu.my) and Mohammad Tariqul Islam (tariqul@ukm.edu.my)

This work was supported by the Universiti Kebangsaan Malaysia (UKM) under Grant AP-2017-007/1.

ABSTRACT A novel, low cost, and comprehensive microwave imaging (MWI) system is presented for the detection of unwanted tumorous cells into the human breast. A compact metamaterials (MTM) artificial magnetic conductor (AMC) surface-inspired coplanar waveguide fed (CPW-fed) microstrip antenna is developed for MWI applications. The initial wideband CPW antenna is designed by the modified oval shape patch and half cycle copper stripe line ground. The antenna is incorporated with two layers uniplanar AMC structure which is composed of a 5×5 array of square modified split ring resonator unit cells to obtain the desired antenna characteristics for the MWI applications like breast imaging. The metamaterial-based AMC structure improves the gain about 5 dB and produces stronger directive radiation characteristics. The enhancement of CPW performance proofs the effectiveness of the double layer MTM-AMC structure and its suitability for MWI. A microcontroller-based PC controlled alternative mechanical imaging system is designed to collect the scattering signal from the CPW-fed antenna. The changes of reflection and transmission coefficient with the variation of dielectric content into the breast phantom structure are analyzed. The remarkable deviation of scattered field is processed by image processing program using Matlab. By using these AMC inspired CPW-fed antenna based microwave imaging, the system can clearly detect the tumor inside the breast phantom.

INDEX TERMS CPW, microwave imaging, artificial magnetic conductor, MTM, breast tumor.

I. INTRODUCTION

Breast cancer is reported as a major cause of death for women all over the world. More than 1.8 million new breast cancer cases are diagnosed every year worldwide. It is due to the presence of malignant cell inside the breast tissue [1]. The key factor of breast cancer treatment is to reliably diagnose it in the earlier stages. Given early breast cancer detection and treatment, the survival rate can even reach up to 97%, which emphasizes the urgent requirement of a reliable and highly efficient method for early breast cancer detection [2]. Over the last few decades, several non-invasive clinical imaging technologies have been proposed to produce the valuable interior pictures of the human body. X-ray mammography, Computed Tomography (CT), Ultra-Sound (US), Magnetic Resonance Imaging (MRI) are frequently used diagnostic tools for detecting breast cancer [3], [4]. However, X-ray mammography produces a relatively high number of false negative diagnoses (between 10% and 30%) and false positive diagnoses (more than 5%). Furthermore, this technique employs radiation and requires uncomfortable compression of the breast during the examination; which yields limited success for patients with dense breast tissue.

Additionally, it is proved that the ionization initiated from X-ray mammography [3] has several health hazards, which paradoxically includes the possibility of turning healthy tissue malignant. The US is a common alternative to breast tumor detection, with a higher (About 17%) false negative rate. Additionally, the deep-lying or solid cancerous tissues

TABLE 1. Comparison of diagnostic performance of different breast tumor detection techniques [6].

Modality	Sensitivity (%)	Specificity(%)	Predictive Value (%)	Accuracy (%)
Mammography	67.85 (120/177)	75.0 (61/81)	85.75 (120/140)	70.20 (181/258)
Clinical examination	50.30 (89/177)	92.0 (75/81)	94.0 (89/95)	63.65 (164/258)
Ultrasound	83.0 (147/177)	34.0 (28/81)	73.50 (147/200)	67.80 (175/258)
Clinical examination & Mammography	77.45 (137/177)	72.0 (58/81)	58.65 (137/160)	75.60 (195/258)
Mammography & ultrasound	91.50 (162/177)	23.0 (19/81)	72.30 (162/224)	70.20 (181/258)
Mammography, clinical examination and ultrasound	93.25 (165/177)	22.0 (18/81)	72.45 (165/228)	70.9 (183/258)
MRI	94.50 (167/177)	26.0 (21/81)	73.60 (167/227)	72.95 (188/258)
Mammography, clinical examination, MRI	99.4%(176/177)	7% (6/81)	70.1% (176/251)	70.5% (182/258)

are difficult to detect. The Magnetic Resonance Imaging (MRI) provides high-resolution images. Furthermore, the cost is very high and it is a time-consuming diagnostic process.

In literature [5], total 258 patients are studied, where 177 with malignant tumors and 177 were with benign tumors. Sensitivity (ratio of detected malignant tumours to the total patient with malignant tumours), specificity (ratio of detected benign tumours to the total patient with benign tumour), positive predictive value (ratio of correctly detected positive malignant tumours to the total positive diagnoses) and accuracy (the ratio of total patient diagnosed benign or malignant tumours to the total patients) are studied to test the present detection techniques. The comparison of the performance of different detection techniques presented in the literature [5] and [6] is presented in Table 1.

The table shows that the percentage of correct diagnosis techniques suffer from limitation. The highest sensitivity, 94.4% was obtained by combining the mammography, magnetic resonance imaging (MRI) and some clinical approaches. The maximum accuracy obtained 75.6%, which proves that each of every four diagnoses is falsified.

For this, an efficient, low cost, nonionizing, portable and comfortable approach is greatly demanded as a complementary tool to the currently applied technology [7]. Nowadays, microwave imaging (MWI) system becomes hot topics of investigation for both as complementary tools and alternative solution of available techniques. It is to overcome the drawbacks in terms of false indication, low-resolution scan, higher cost and uncomfortable process. Microwave imaging has advantages of high positive rate, low cost, comfortable, high data-rate, lower complexity, portable and very low power density. The basic principle of MWI is to analyze the change of the back-scattered signal with the change of different electrical properties of tissues. The antenna plays an important role in microwave imaging. In MWI, antennas are used as a transceiver to impinge the microwave signals on human tissue [8]. The remarkable variation of the back-scattered signal can exploit the unwanted tumor cells inside the breast which contain higher dielectric constant than normal breast tissues [9], [10]. From recent studies to use the antenna as a transceiver in MWI should meet the different criteria [11]–[13] like high gain and small in size; Directive radiation of power; Wide range of frequency with higher efficiency; relatively simple in model; Compatible penetration to human tissue; Ability to operate both in low and high frequencies.

Although microstrip antenna is quite simple to design and cost-effective it suffers from a number of limitations including low gain (<5 dBi) and weak in radiation performances. A number of techniques are proposed by several researchers to obtain higher gain, wider bandwidth and directive characteristic of microstrip antennas. Some of these are use of unit-cell antenna [14], Cross Vivaldi antenna [15], metamaterials (MTM) antenna [16], slot loaded antenna [17], incorporating electromagnetic structures [18], metallic backed artificial magnetic conductor (AMC) [19] etc. These techniques made the antennas compatible with MWI system.

The introduction of MTM has created a-new-era in microwave imaging (MWI) application due to its great potentials for the implementation of microwave devices. A negative-index MTM is ''an engineered electromagnetic structure with extraordinary properties which are generally not found in nature''. By using these metamaterial features, MWI devices such as antennas are developed which have exterior properties in terms of wavelengths, controlling of wave beams, permittivity, permeability etc. These features made MTM antennas a great interest in medical applications. The study of metamaterial has been expanded by adopting various techniques such as SRRs [20], [21], structure based on transmission line [22], resonators of double-bowknot shape [23], complementary electric field-coupled resonator [24]. Due to miniaturization, cost-effectiveness and the capabilities of label-free detection, metamaterial based antenna has been focused on the design of MWI system [25].

Artificial Magnetic Conductor (AMC) is a promising tool to enhance the antenna performance such as gain, directivity, bandwidth and radiation performance. AMC is an artificially engineered periodically loaded structures which are used to stop the propagation of antenna in a specific direction or reducing backward radiation called phase reflection. The Phase reflection causes due to an artificial magnetic conductor which is not readily available in nature. Different forms of AMC structure are found to improve the antenna performance in terms of gain, directivity and radiation efficiency [26]–[28]. Among them, the uniplanar structure is very

common because of its simple configuration and suitability of different microwave application. Bandwidth enhancement is reported in [29] and [30] by using CPW-fed dual band antenna and uniplanar AMC combination but expense the space. A triangular shape CPW-fed antenna is combined with an electromagnetic reflector to widened the lower and upper bands [31]. Though radiation efficiency is improved, but gain does not improve remarkably. The bandwidth and gain enhancement of a high-frequency CPW-fed antenna is presented in [32] where an unlicensed band (60 GHz) antenna is proposed using I shaped slot uniplanar-compact (UC) electromagnetic structure. A coplanar waveguide-fed multiband antennas with and without uniplanar copper strip-based electromagnetic band gap (CS-EBG) structure is presented for portable Multiband wireless applications [33]. The antenna, when combined with the CS-EBG structure, still preserved its multiband characteristics although resonance was shifted and produced near directional pattern because of the reflecting property like AMC of the CS-EBG/AMC structure behind it, which was donut and omnidirectional shape in case of the antenna alone. Therefore, the combination of uniplanar AMC structure with wide band microstrip antenna is still an issue of a challenge to achieve higher gain and directivity. A compact periodic AMC surface structure with higher gain and the unidirectional radiation pattern is required for implementation of MWI applications.

This work presents a new, modest, complete and comprehensive microwave imaging system to detect the unwanted tumorous cells into the human breast. Firstly, a CPW-fed microstrip antenna with modified oval shape patch is designed for UWB band. Then, a new two-layer uniplanar AMC structure of 5×5 array MTM unit cell is combined with CPW-fed antenna to achieve desired properties for microwave imaging application, especially for breast imaging. By using the AMC surface structure gain of CPW-fed microstrip antenna is increased about 5 dB and made the antenna more directive with lower interference to adjacent microwave elements. An automated PC controlled microwave imaging system is developed. The AMC inspired CPW-fed antenna is used as a transceiver in breast imaging model. Commercially off-the-shelf breast phantom containing dielectric properties same as real breast tissue with the inclusion of tumor cell is used for experimental validation. The change of backscattered signals with the change of dielectric content inside the structure of breast phantom is analyzed. The remarkable variation of scattered field is an important issue for breast phantom scanners. The variation of scattered field is processed by image processing program using Matlab. By using the modified CPW-fed antenna, the microwave imaging system can localize the tumor or unwanted cell inside the human breast.

II. UNIT CELL AND AMC DESIGN ARCHITECTURE

The proposed AMC inspired CPW-fed antenna design starts with a metamaterials unit cell. The desired goal of the unit cell is to attain resonance within the frequency band 3-10 GHz for

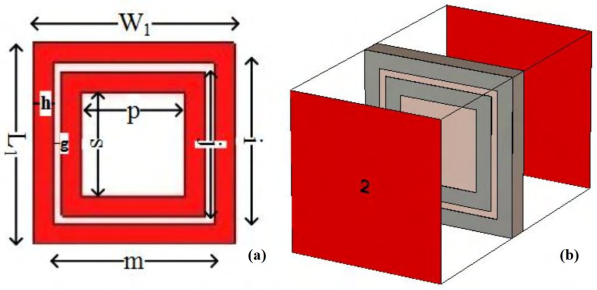

FIGURE 1. (a) Proposed MTM unit cell (b) Simulation setup of proposed unit cell.

microwave imaging. The design view of the proposed planar square unit cell is shown in figure 1(a). The size of the unit cell is 12×12 mm^2 with comprised of two copper strip rectangular ring patch with different size. The parameters of the unit cell are optimized and adjusted so that AMC structures resonance and a resonance of CPW-fed microstrip antenna be close. Ideally, a period of AMC structure length should smaller than $\lambda/2$. For the resonant, at 6.12 GHz the value is 24 mm. By introducing the inner rectangle and optimizing the gap between copper stripes the proposed AMC size is compact within 12 mm. The design parameters of unit cell are given below: W1=L1=12 mm, m=i=9.6 mm, j=8.6 mm, s=p=6.20 mm, h=1.20 mm, g=0.5 mm.

The finite element method based HFSS simulator is used to investigate the design to calculate scattering parameters. The structure is placed inside the two waveguide ports on the positive and negative z-axis. Figure 1(b) shows the simulation setup of unit-cell. The S-parameters of proposed unit-cell (reflection coefficient (S_{11}) and transmission coefficient (S_{21})) is depicted in figure (2). The proposed MTM unit-cell is polarization independent and transparent to a frequency band centered at 5.35 GHz with half power (3-dB) bandwidth of 1.5 GHz. The resonance at 8.25 GHz in the transmission coefficient (S_{21}). The self-resonance, the overlap, and larger overall current responses proof the effectiveness of metamaterials magnetic response. The proposed uniplanar copper strip based artificial magnetic conductor (CS-AMC) structure is designed using an array of identical unit cells. The arrangement is in two different layers using two different substrate materials. The CS-AMC structure is shown in figure 3.

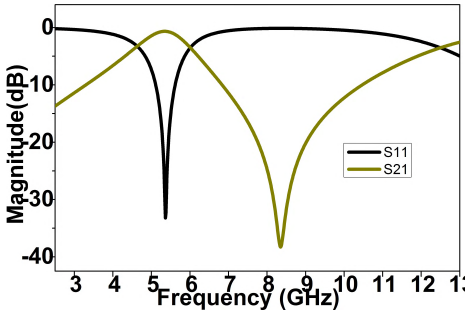

FIGURE 2. The magnitude of S-parameters of proposed unit cell.

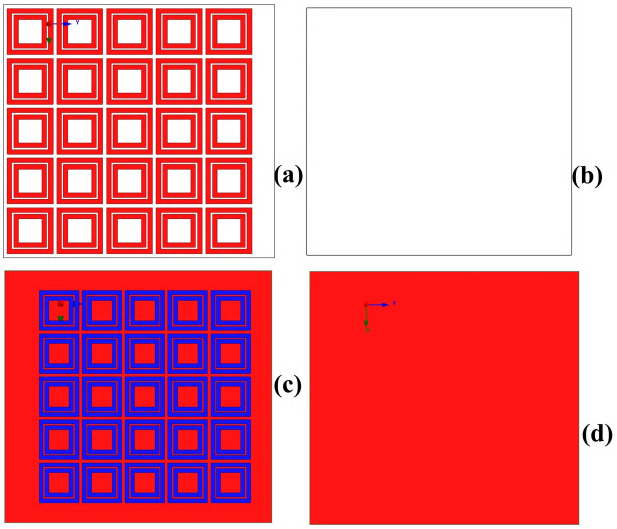

FIGURE 3. (a) CS-AMC inner layer top (b) CS-AMC inner layer bottom (c) CS-AMC outerlayer top (d) CS-AMC outer layer bottom.

Each structure is composed of a 5×5 array of unit cells with each unit cell size of 12×12mm^2. The dimension of the inner layer is 66×66 mm^2 using Rogers RO4003C substrate thickness 0.2mm with dielectric constant of 3.55. There is a 1mm gap between each unit cell. The outer layer structure is realized by placing the array on a 76×78 mm^2 FR4 substrate of 1.6 mm thickness with dielectric constant of 4.6. These substrates are commercially available, low cost and easy to fabricate the multilayer PCBs. These two layers are placed as they become offset to each other. This is a new technique to obtain multiple resonant using simple and compact uniplanar structure to comply with the objectives. The tuning of both copper strip rings and the gap between them are used to attain the band gaps around the resonance or unattainable stop band of CPW. The structure act as an artificial magnetic conductor (AMC) characteristic at different frequencies where it shows inherent in-phase reflection properties. The transmission characteristics are verified by placing the AMC structure in between two waveguide ports. The reflection (S_{11}) and transmission (S_{21}) characteristics of proposed AMC structure are shown in figure 4. The transmission peaks occur at frequency 4.4 and 9.3 GHz. The half power (3-dB) bandwidth of array is same as a unit cell and transparent to a frequency band centered at 5.35 GHz. There has an extra resonance in the array structure after 9 GHz which is out of considering CPW band. In a 5×5 array, the frequency is shifted downward.

III. CPW ANTENNA WITH AMC STRUCTURE: DESIGN APPROACH

At first, an antenna is designed with the coplanar waveguide (CPW) fed line. The antenna is fabricated on commercially available FR4 material with the thickness of 1.6 mm having a dielectric constant of 4.6. FR4 is commercially available low-cost material and convenient to make multilayer PCBs. The prototype was designed with modified oval shape patch and

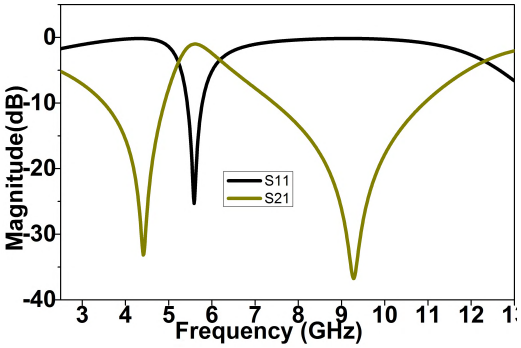

FIGURE 4. The magnitude of S-parameters of 5×5 array configuration.

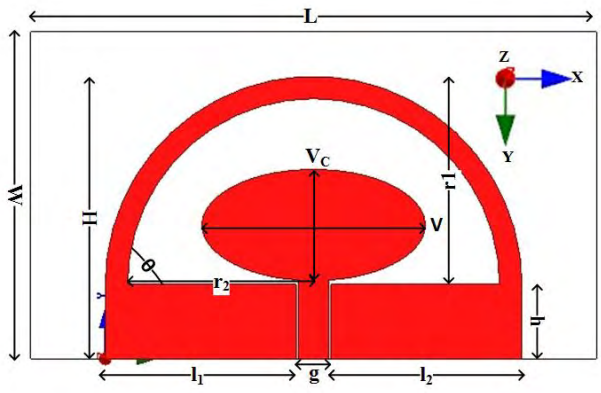

FIGURE 5. Geometric layout of CPW-fed antenna.

coplanar ground plane. The ground plane has a half cycle copper strip line on it. The geometric layout of CPW-fed antenna is shown in figure 5. The overall size of proposed CPW is 76×44 mm^2. The major radius (V) and minor radius (V_c) of oval shape patch is 30 mm and 15 mm with area πVV_c. The width (g) and height (h) of fed the line is 4 and 10 mm. Overall height of coplanar ground (H) is 38 mm and length of each rectangle ($l_1 = l_2$) is 25.5 mm. The gaps between feedline and ground rectangles are 0.5 mm. This gap is to obtain wider bandwidth. A positive half cycle of 28 mm (r_1) radius is taken on ground plane and another inner cycle with 25 mm (r_2) is etched away from outer cycle to create the 3 mm copper stripe line. The copper strip has strong effect to increase the antenna electrical length in both the lower and upper operating frequency.

The elementary goal of this AMC inspired CPW-fed antenna is to exploit the difference backscattering signal based on the complex dielectric constant of breast tissues. For microwave imaging applications, the antenna should meet some criteria like higher gain, wideband, sharp resonance frequencies, and directional radiation. These are important to scan the deeper tumor with high-resolution images [34]. Generally, the multilayer surface structures antenna is used in to obtain smooth radiation-profile, to minimize the back-radiation, to get improved gain and efficiency than conventional microstrip antenna. After completing the proposed AMC structure, the final step is to implement the previously

designed CPW-fed antenna. The final CPW-fed microstrip antenna is formed by using the CPW-fed radiator as a top layer above the AMC surface. The final formation is depicted in figure 6. The cavity between the layers is 6 mm. M_3 flat head nylon screw is used to form the layers with the cavity. The antenna radiation performance, directivity,and front to back ratio are improved by using the phase reflection property of AMC structure. A 50Ω SMA connector is used to feed the CPW antenna. The SMA connector has 2.08 dielectric permittivity and 4.62×10^4 S/m electrical conductivity.

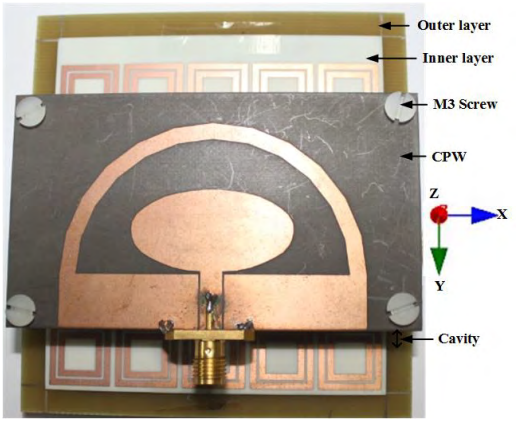

FIGURE 6. Proposed CPW-fed antenna prototype.

IV. ANTENNA PERFORMANCE ANALYSIS

The performance characteristics of the AMC inspired CPW-fed antenna has been analyzed, studied and optimized by utilizing the 3D electromagnetic structure solving functionality of ANSYS' FEM (finite element method) based HFSS simulator. The completion of parametric studies gives the optimized geometric layout of the prototype which is developed through an in-house fabrication process (PCB-LPKF machine) to fabricate the physical model. The measurement process was performed by using an Agilent E8362C VNA which covers the frequency range starting from 10 megahertz to 67 Gigahertz and Satimo near-field-measurement lab (UKM StarLab) which use the software satimo passive measurements (SPM) and SatEnv. The measurements setup are presented in figure 7(a&b).

The results of the simulated and measured reflection coefficient for the realized antenna are depicted in figure 7(c) & (d). From the measurement results, the CPW-fed antenna impedance bandwidth is 4.5 GHz from 3.1-7.6 GHz with two resonant at 3.6 and 6.5 GHz. When the AMC structure is used as reflector the antenna impedance bandwidth is broadened in both sides. The lower band is enlarged by 200 MHz and the upper band also preserved 300 MHz more bandwidth. The AMC inspired CPW-fed is operated around 3, 4 and 6.15 GHz with preserving more 6.66% coverage (2.9-7.8 GHz). The CPW and AMC combination creates a new resonant at 4 GHz and other resonant are shifted to left because of the capacitive effects generated between the CPW and CS-AMC structure. Another remarkable point is the large decrease in the magnitude of return loss is obtained after combining the CS-AMC structure. In CPW it mostly decreases to about -22 dB whereas with CS-AMC structure is about -28 dB. There have no gap or mismatch in the entire bandwidth. The simulated and measured resonant frequencies are well agreed (Figure 7(d)) and a small deviation has found due to the fabrication tolerances. The simulated and measured peak realized gain is presented in figure 7(e). The peak gain is about 10 dBi which is better than recently published UWB antenna. The uses of AMC structure promote the optimal conditions for the main radiator to avoid trapping. The radiation characteristics are improved by the AMC structure due to control of the current distribution by reducing energy leakage near the lateral antenna edges. The peak realized gain of proposed CPW-fed antenna for both in with and without AMC structure is shown in figure 7(f). By using the AMC structure gain of CPW-fed microstrip antenna is increased about 5 dB and made the antenna more directive with lower interference to adjacent microwave elements. The gain was around 4-6 dBi in normal case whereas it rises to around 8-11 dBi in the final design. There has few changeability in gain level because two different kinds of structure are combined and made a single one. The enhancement of CPW performance proofs the effectiveness of double layer AMC surface structure and its suitability for MWI applications. Figure 7(g) depicts the simulation and measured radiation efficiency. The proposed prototype offers radiation efficiency greater than 82% over the operating band which is better than the antennas presented in the literature. By using the AMC surface the antenna becomes more directive with lower interference shown in figure 7(h). The directivity is enlarged about 4 dB.

The phase distortion of the transmitted signal over the transmission path is represented as group delay. It is the negative derivative of phase response with respect to the frequency. The group delay of the proposed prototype at a distance of 200 mm in both the face to face and side by side orientation is presented in figure 8. In side by side orientation, it is higher than that of face to face orientation. In face to face, it is almost linearly distributed except a single pick at 4.8 GHz. In face to face orientation, the antenna can radiate short pulses with very small distortion and minimal late time ringing. Only the pulse has spread slightly. Due to the directional characteristics of the antenna, the transmitted signal is spread in a single direction. For this, the antenna is recommended to use in face to face orientation for microwave imaging.

The fidelity factor is determined by the highest magnitude of cross-correlation among the transmitted and received signal. If the τ is the transmission delay than the correlation factor is defined by the following equation:

$$F = \max \frac{\int_{-\infty}^{+\infty} x(t)y(t-\tau)dt}{\sqrt{\int_{-\infty}^{+\infty} |x(t)^2| dt \int_{-\infty}^{+\infty} |y(t)^2| dt}} \quad (1)$$

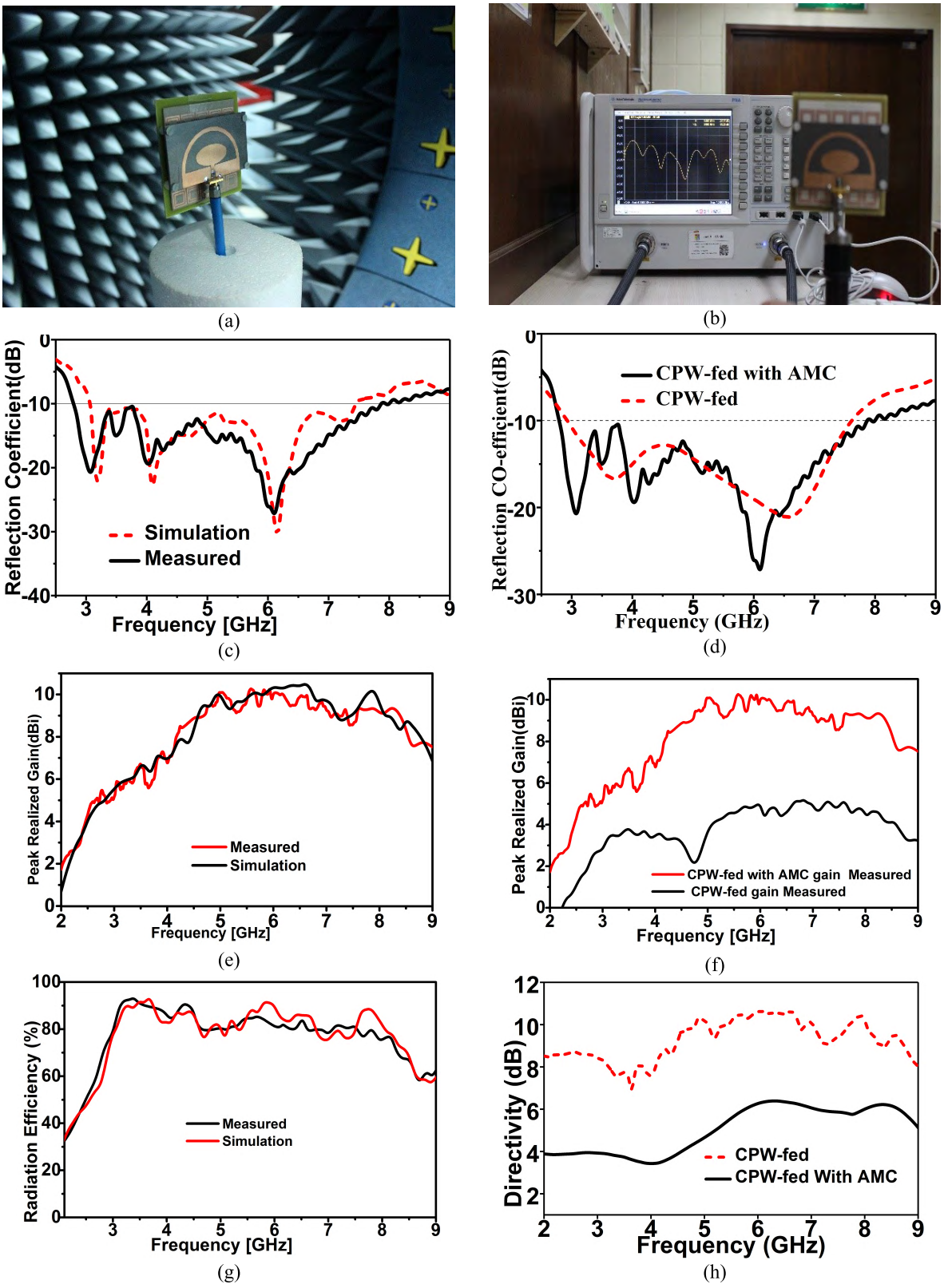

FIGURE 7. (a) Fabricated prototype with measurement setup at the satimo lab (b) Reflection coefficient measurement setup with VNA (c) Reflection coefficient of proposed antenna prototype (d) Comparison of reflection coefficient of CPW-fedantenna with and without AMC structure (e) Measured and simulated realized gain of proposed antenna prototype (f) Gain comparison of CPW-fed antenna with and without AMC structure (g) Measured and simulated radiation efficiency of proposed antenna (h) Directivity of proposed prototype with and without AMC structure.

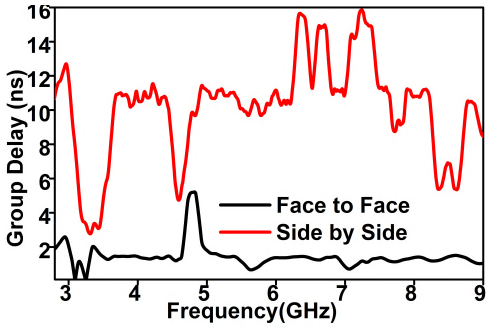

FIGURE 8. Group delay of proposed prototype.

Where, the transmitted (TX) and received (RX) signal are represented as x (t) and y (t) respectively. In both cases ($f_{to}f$ and $s_{by}s$) antennas are placed at a distance of 200mm from each other. Matlab is used to develop the fidelity equation and calculate its value. For face to face orientation, the fidelity factor is 0.91 whereas for side by side is 0.42 respectively. The fidelity factor of the proposed antenna in the face to face orientation is more novel than recently published CPW antennas. The higher value of fidelity factor guarantees the lower distortion of the transmitted signal. This attribute confirms that the antenna is suitable to use for microwave imaging.

The simulated radiation pattern of CPW antenna and antenna with AMC structure in *xz* (phi 0) and *yz* (phi 90) plane is shown in figure 9. As discussed earlier, the AMC structure reduced the back radiations and directed the radiations to broadside direction. It is observed that the CPW antenna with AMC structure shows more directive radiation as compared to CPW-fed antenna. The use of proposed AMC, the power along bore side is increased. The surface waves are reduced by the structure. This proves that the application of AMC improves the radiation characteristics, gain, directivity etc.

The measured radiation pattern in major planes for resonant frequencies is depicted in figure 10. In Satimo measurement lab (UKM StarLab) antenna is measured according to Phi axis rolling and Theta stepping. Measurements are logged in tables of Theta and Phi spherical coordinates. The spherical coordinates relate to the Cartesian axes as follows: XZ Cut is Theta=0 to 360 & Phi=0, YZ Cut is Theta=0 to 360 & Phi=90 and XY Cut is Theta=90 & Phi=0 to 360. The xz-plane (φ=0) and yz-plane (φ=90) are considered as E-plane and *H*-plane. The near-field performance shows that the use of proposed AMCstructure made the antenna unidirectional. The main lobes direction is fixed to the broadside radiation which improves both the E and H-plane radiations. The radiation patterns of CPW-fed antenna is mostly bi-directional, whereas using AMC the antenna is maximized along broadside at 0°. The antenna directivity is increased about 4.5 dB. The front-to-back ratios with AMC structure are about 20 dB, 25 dB and 32 dB at 3.1 GHz, 4.05 GHz and 6.1 GHz respectively. Another remarkable feature is very small back lobe is introduced. In higher frequency, especially in more than 6 GHz there exist few nulls in the radiation

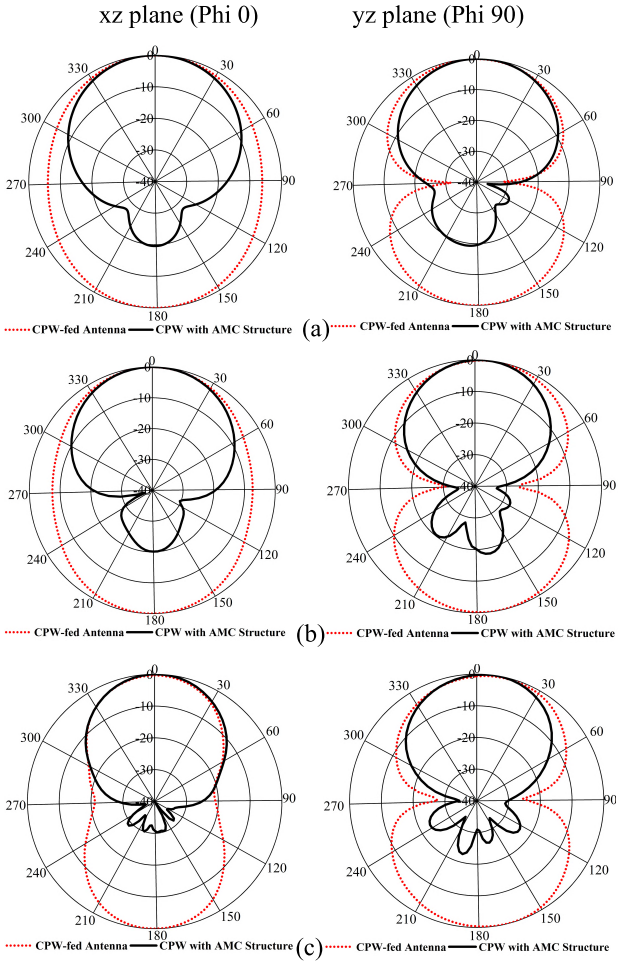

FIGURE 9. The simulated Radiation pattern of with and without AMC structure at (a) 3.1 GHz (b) 4.05 GHz (c) 6.1 GHz.

patterns because of higher order excitation [35]–[37]. From the discussion, the-use-of AMC structure reduces the energy leakage of CPW-fed antenna because of its reflecting property.

The Surface-current distributions at resonance frequencies of CPW-fed antenna with and without AMC structure are shown in figure 11.

The main current conducting area of CPW-fed antenna is around the feedline and the copper stripe of the co-planner ground. At higher frequency, the surface current is evenly raised over the oval of the patch. It is observed that the used AMC structure minimize the spreading out of feedline current. The fedline current is well-suppressed by the CS-AMC cells. The fedline current mostly expenses to energized the antenna radiating patch. The edge-to-edge coupling between the patch and the ground aid to create an extra radiation. The AMC structures block the surface wave along the horizontal cut which assists to improve the mutual-coupling between elements.

V. MICROWAVE IMAGING

The ultimate target of our system is to retrieve the change in terms of backscattering signal with present some high

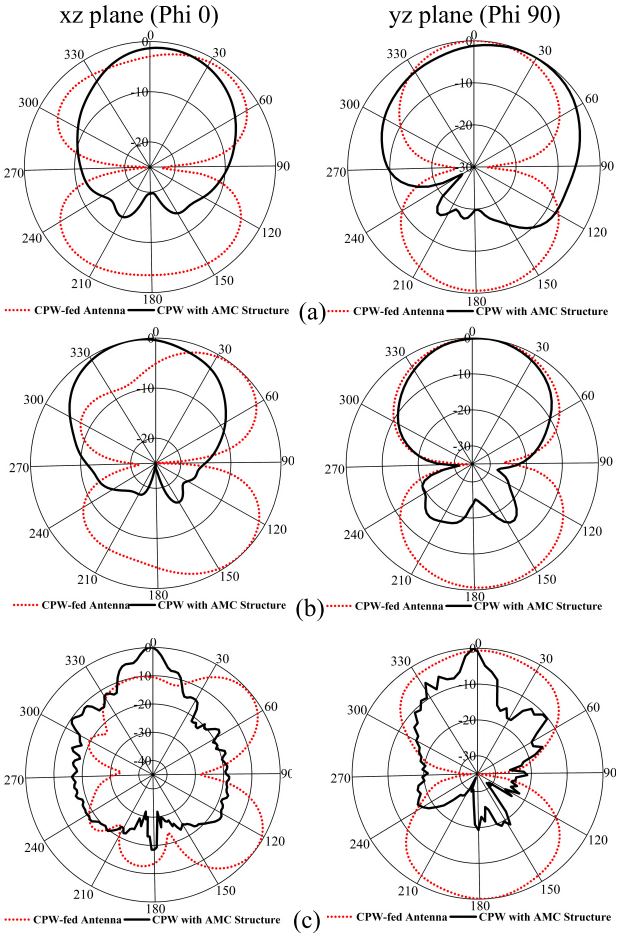

FIGURE 10. Measured Radiation pattern with and without AMC structure at (a) 3.1 GHz (b) 4.05 GHz (c) 6.1 GHz.

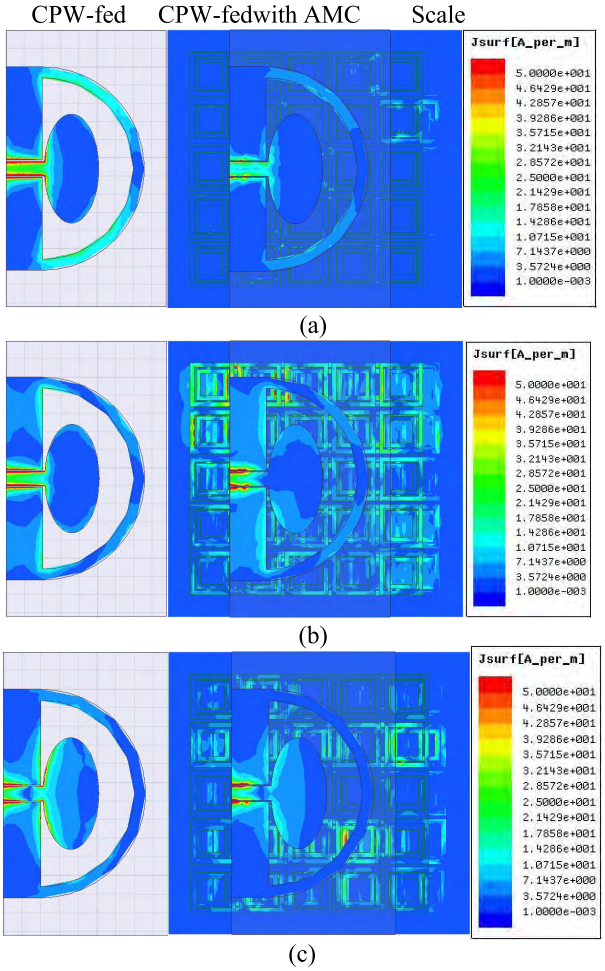

FIGURE 11. Surface Current Distribution for with and without AMC structure at (a) 3.1 (b) 4.05 and (c) 6.1 GHz.

dielectric inclusion as a tumor. We applied two commercially available off-the-shelf homogeneous breast phantoms from Japan with single tumor of higher dielectric constant. One is transparent and another is opaque shown in figure 12 (b). The phantom is of 160×80 mm^2 size containing nearly standard dielectric properties as a human breast. The Phantom consists of four layers. These are the skin layer, the breast tissue layer or fat, cancer benign breast tumor and the normal air layer. The experimental skin layer has following characteristics: dielectric constant = 38, thickness = 2.5 mm, and conductivity = 1.49 S/m. The thickness of breast tissue layer is 8.75 mm with permittivity 5.14 and conductivity 0.141 S/m. The cancer benign breast tumor part have dielectric constant = 67 [38], [39] with 10 mm diameter. The tumorous cells are normally high water content whose dielectric constant is higher compared to low water tissues such as fat [40], [41]. For experimental setup, we have designed an automatic microwave imaging system shown in figure 12(a). Two CPW-fed antenna is placed face to face at a distance of 18 cm. The phantom is placed inside these antennas on a rotating platform. The mechanical rotation platform can rotate the antennas in polar coordinates from 0 to 2π using a stepper motor. The rotation is controlled using an Arduino Uno control circuit. The stepper motor is step by 3° and total 360° is divided into 120 equivalent points. Each antenna maintains a specific distance of 6.5 mm from breast phantom. The antenna is connected to a Vector Network Analyzer (VNA Agilent N5227A) to collect the antenna scattering signal. All these devices and electromechanical circuits are controlled by a single PC which is connected to Arduino control and VNA using GPIB port.

The experimental setup of proposed microwave imaging system is shown in Figure 12(c). We don't use any human body or patient in this case due to the safety permission which is ongoing. For laboratory test, we rotate the phantom to take data all around the phantom to localize the position of the tumour. In final system, the rotation platform will be set up as it will work as medical imaging bra which will rotate clockwise. The breast phantom is placed between two antennas and the effects of the breast tissues are studied on the performance of the antenna. The VNA parameters are set as IF bandwidth 10 HZ, 10 dBm output power, and 3.1 to 7.6 GHz frequency range. The transmitting antenna transmits the microwave pulse towards the breast phantom and the receiving antenna receives the scattering signals reflected from the phantom. To mitigate air-interference the entire

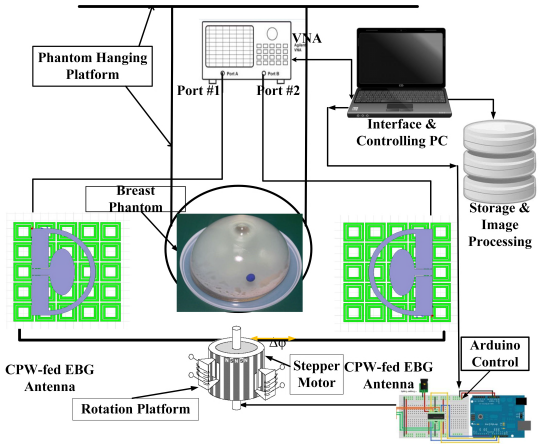

(a)

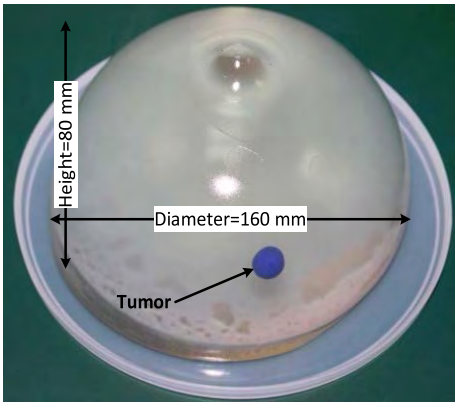

(b)

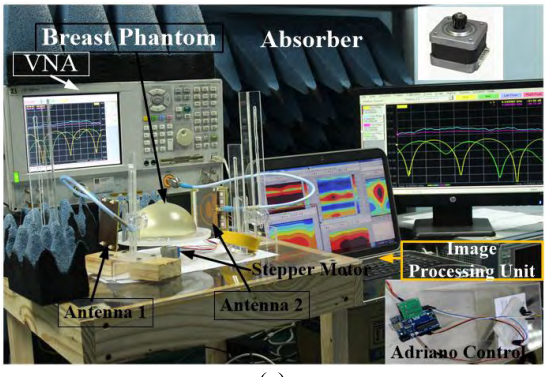

(c)

FIGURE 12. (a) Block diagram of imaging system (b) Breast phantom (c) Experimental setup.

system is calibrated over the operating frequency using SOLT calibration (3.5 mm Agilent 85052 D) kit. By using measurement setup, the complex frequency domain scattering (S_{11}, S_{21}, S_{12} and S_{22}) parameters Γ (φ_n, f_m) are measured over the operating frequency band, where m = 1, 2 . . . .M (M=201) and n = 1, 2 . . . ..N represent the angular positions of each rotation. The transmitted parameters rely on the entire path between the two antennas, which the tumor crosses twice during the complete rotation. The reflected parameter mostly presents the shallow depths under the skin layer as signals are bounced off the opposite side of the breast phantom should travel through the phantom twice and are significantly attenuated. The antennas with high gain and very low inherent return loss with directive nature can perfectly detect reflected signals. The measured data were processed with Delay-Multiply-and-Sum (DMAS) algorithm [42] and reconstruct the image of internal breast phantom structure. In DMAS algorithm reconstructed image highlights the electromagnetic scattering rather than recovering the dielectric profile. The frequency domain data of reflection co-efficient is converted to time domain for each antenna using inverse discrete Fourier transform.

For more clearer and sharp image of breast interior the blind-deconvolution method is used, where the point spread function (PSF) is optimized using latest heuristic optimization algorithms [43]. The deconvolution techniques rely on PSF which is reliant on orientations and near-filed patterns of antennas. The PSF describes a single pixel in the ideal image and reproduced the others than a single pixel in the real image. For a linear imaging system, the image of an object can be expressed as [42]:

$$\mathrm{g(x,\,y)} = \int_{-a}^{a}\int_{-a}^{a} h\,(x, y; \alpha, \beta) f\,(\alpha, \beta)\, d\alpha\, d\beta + \eta(x, y) \quad (2)$$

Where, $\eta(x, y)$ is the additive noise function, $f\,(\alpha, \beta)$ is the object, g(x, y) is the image and h is the point spread function. The ";" is used to distinguish the input and output pairs of coordinates. The $h\,(x, y)$ is given as:

$$h\,(x, y) = \frac{i\omega\rho\vartheta_o}{4\pi^2} H\,(z_o, x, y)\,\frac{\partial}{\partial z} H\,(z, x, y)\,|_{z=z_o} \quad (3)$$

Where

$$H\,(z, x, y) = \frac{i2a}{k}\int_0^{\pi} d\varphi \frac{scos\varphi - a}{s^2 + a^2 - 2ascos\varphi} \times \left(e^{-ik\sqrt{s^2+a^2-2ascos\varphi+z^2}} - e^{-ikz}\right) \quad (4)$$

$s^2 = x^2 + y^2$, a is the radius of the transducer area, ϑ_o is the velocity amplitude and ρ is the density of the medium.

The tumor is clearly detected by differentiating the collected scattering signal from the healthy and unhealthy tissue of breast phantom. Because of the high dielectric properties of tumorous cells, the reflected signal is bounced off and changes the S-parameters. The total process of the experiment is done with single run command and takes total 6 minutes to complete single scanning.

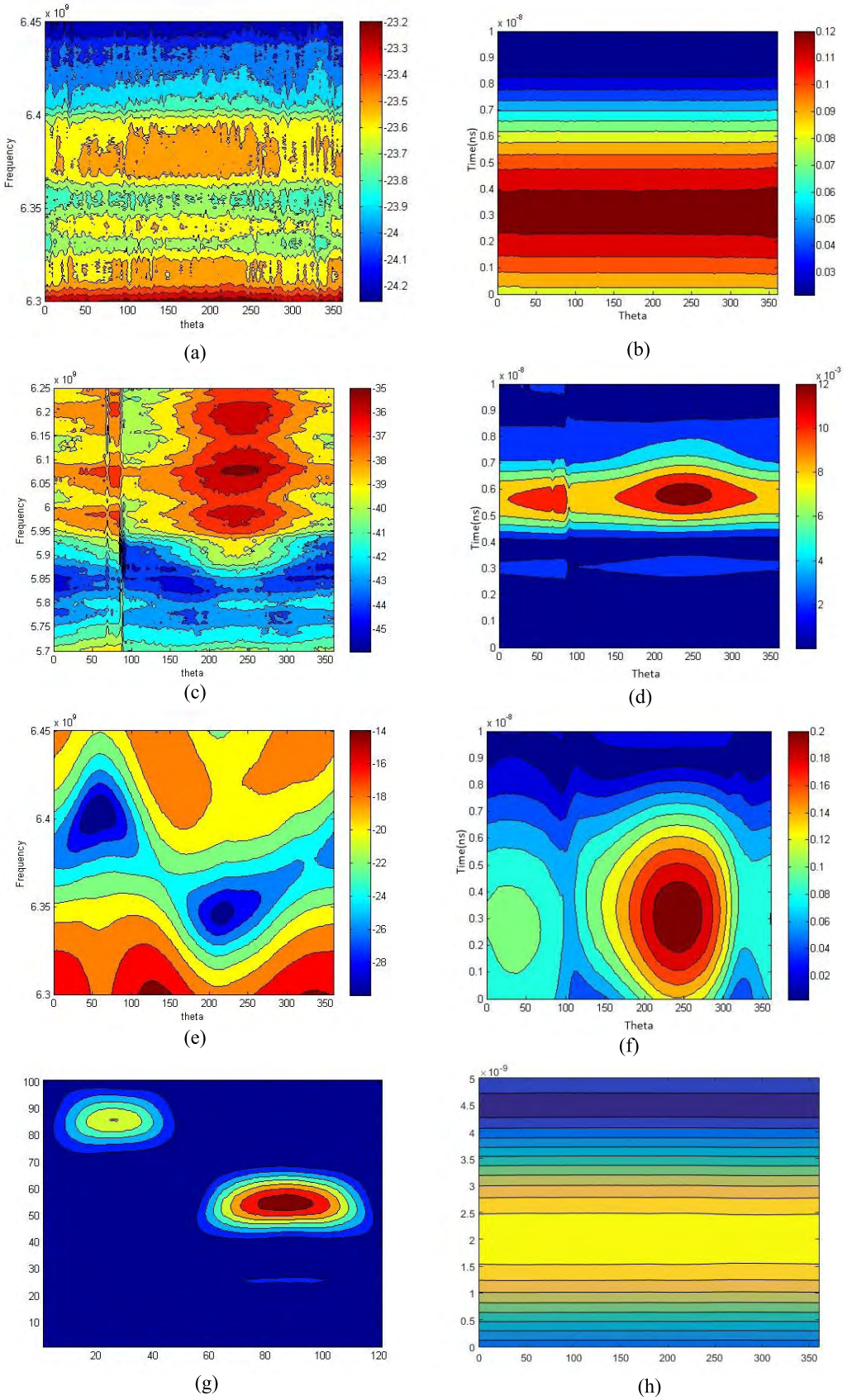

FIGURE 13. (a) Frequency domain output without tumor (b) Time domain output without tumor (c) Frequency domain output with tumor in transparent phantom (d) Time domain output with tumor in transparent phantom (e) Frequency domain output with tumor in opaque phantom (f) Time domain output with tumor in opaque phantom (g) Image after blind deconvolution for transparent phantom (h) Time domain output in free space.

TABLE 2. Comparison of proposed system performance with some existing system.

System	Imaging Domain	Antenna Configuration	Targets	Results
Proposed system	Commercially available off-the-shelf breast phantom	Two Compact AMC inspired CPW-fed microstrip Antenna	To detect the unwanted tumor cells inside the breast	Portable, compact, low-cost system with required image processing mechanism tested with artificial breast phantom and validate to earlier breast tumor detection.
[10]	Numerical tumor models	Not mentioned	Numerical investigation of microwave backscatter to classify the salient features of a dielectric target.	The target can be classified directly from its UWB backscatter.No real physical system presented, only (FDTD) method formulated as a 3-D total-field/scattered-field (TF/SF) problem.
[11]	Hemispherical breast phantom	16-element a hemispherical array of bowtie antenna	3-Dimensional (3D) detection of a breasttumor.	Able to detect a tumor.Complex, bulky and non- portable system.
[12]	Scattered fibroglandular	32 dual-band miniaturized patch antennas	Comparing 3-D quantitative microwave breast imaging performance	The results suggest that these miniaturized antennas are suitable candidates for multiband microwave breast imaging systems. No real system presented, only simulated data were processed.
[13]	Simulated CAD model	An array of 16 antennae.	A sample image from a phantom experiment.	The antenna to radiate a broadband pulse into the breast, and the antenna is shown to perform well. No image processing mechanism presented.
[34]	A semi-spherical breast phantom	Two cavities backed Vivaldi antenna	Reveal the sense to the scattered field of the small dielectric inclusions inside the breast phantom.	Change of amplitude and phase for the tumor and the metallic object. The absence of image processing and presenting mechanism.
[44]	Realistic anthropomorphic breast phantom	5 uniplanar elliptical antennas	In-depth inspection of breast tissues.	Analyze the change of scattering parameters due to presence and absence of tumor. Lack of post-processing to present the scattering parameter to present visibility of tumor.
[45, 46]	Acrylonitrile butadiene styrene plastic half sphere	UWB radar	Measure the symptomatic patients	First real breast phantom but limitations in terms of resolution and clutter rejection.
[47]	Rectangular tub with cooking oil	UWB Vivaldi antennas	Breast cancer/tumor detection	Detect 9 mm metallic ball. No real breast phantom was tested.
[48]	Water filled spheres	32 monopole antennas	20 to 40 mm target objects detection	3D images are obtained by consuming more than 100 minutes
[49]	Hemispherical ceramic(Al_2O_3) radome	16 elements antenna array	Clinical testing	The first study of microwave time domain with volunteers

Figure 13(a) to (h) shows the imaging output of the proposed system using CPW-fed antenna. The breast tumor detection for both transparent and opaque breast phantom in both frequency and time domain is presented. It is observed that the phantom without tumor transferred the signal and has no change or reflection over the path as shown in figure 13(a) & (b). At the time of the experiment, a phantom with tumor it is evident that the tumor is visible at near 250° shown in figure 13(c) & (d).

The variation appears twice in the transmitted s-parameter with another slightly lower power artifact at about 70°. The transmitted parameters rely on the entire path between the two antennas, which the tumor crosses twice during the complete rotation. The artifacts appear after 0.55 ns. This can be translated into the distance from the antenna using the propagation rates in the different media involved. Afterward, when we examined the system with opaque phantom, the proposed prototype can detect the tumor at approximately 240 degrees and a low power artifact at about 55 degrees shown in figure 13(e) & (f). The red color area in time domain output indicates the higher reflection coefficient. The reflection caused by the tumor increase the overall return

loss which causes the more power reflected the antenna as it dissipated within the phantom. Figure 13(g) depicted the blind deconvolution image which makes clearer and sharper the tumor. In a free space, the antenna propagates the signals without any interference and made a homogeneous path over the transmission path shown in figure 13(h). Table 2 lists out the comparison of the proposed system with some existing systems in the literature. The proposed imaging system is smaller insize, portable, compact, low-cost system with required image processing mechanism tested with artificial breast phantom and validate to earlier breast tumor detection. The proposed system achieves much better results than systems reported in the literature and makes it suitable for microwave imaging applications.

VI. CONCLUSION

The AMC characteristics of proposed MTM unit cell are studied and verified for microwave breast imaging. It is established that the-use-of MTM AMC structure enhances the antenna performances especially the gain and directivity. By using the AMC structure, gain of CPW-fed microstrip antenna is increased about 5 dB and directivity is improved about 4.5 dB with lower interference to adjacent microwave elements. The reflection properties of the AMC structure shortened the energy leakage and made the antenna unidirectional. The proposed AMC inspired CPW-fed antenna is used as a transceiver in an automated PC controlled microcontroller based breast tumor detection system. The data acquisition system around the phantom, transmitter, receiver and image processing program using Matlab is developed. The variation of scattering signal due to the variation of dielectric properties of the phantom are analyzed and presented. The system has many advantages e.g. portable, compact, low cost and easy installation. The system is tested with artificial breast phantom. In conclusion, the obtained performance of imaging system support and validate it to a potential candidate for the earlier breast tumor detection in the human breast.

REFERENCES

[1] M. Kahar, A. Ray, D. Sarkar, and P. P. Sarkar, "An UWB microstrip monopole antenna for breast tumor detection," *Microw. Opt. Technol. Lett.*, vol. 57, no. 1, pp. 49–54, 2015.
[2] H. Zhang, "Microwave imaging for ultra-wideband antenna based cancer detection," Ph.D. dissertation, School Eng., Univ. Edinburgh, Edinburgh, U.K., 2015.
[3] C. K. Kuhl *et al.*, "Mammography, breast ultrasound, and magnetic resonance imaging for surveillance of women at high familial risk for breast cancer," *J. Clin. Oncol.*, vol. 23, no. 33, pp. 8469–8476, 2005.
[4] J. G. Elmore, M. B. Barton, V. M. Moceri, S. Polk, P. J. Arena, and S. W. Fletcher, "Ten-year risk of false positive screening mammograms and clinical breast examinations," *New England J. Med.*, vol. 338, no. 16, pp. 1089–1096, 1998.
[5] W. A. Berg *et al.*, "Diagnostic accuracy of mammography, clinical examination, US, and MR imaging in preoperative assessment of breast cancer," *Radiology*, vol. 233, no. 3, pp. 830–849, 2004.
[6] A. M. Hassan and M. El-Shenawee, "Review of electromagnetic techniques for breast cancer detection," *IEEE Rev. Biomed. Eng.*, vol. 4, pp. 103–118, 2011.
[7] H. Bahrami, E. Porter, A. Santorelli, B. Gosselin, M. Popovic, and L. Rusch, "Flexible sixteen monopole antenna array for microwave breast cancer detection," in *Proc. 36th Annu. Int. Conf. IEEE Eng. Med. Biol. Soc.*, Aug. 2014, pp. 3775–3778.
[8] Y. Zhang, W. Hong, C. Yu, Z. Q. Kuai, Y. D. Don, and J. Y. Zhou, "Planar ultrawideband antennas with multiple notched bands based on etched slots on the patch and/or split ring resonators on the feed line," *IEEE Trans. Antennas Propag.*, vol. 56, no. 9, pp. 3063–3068, Sep. 2008.
[9] M. Lazebnik *et al.*, "A large-scale study of the ultrawideband microwave dielectric properties of normal breast tissue obtained from reduction surgeries," *Phys. Med. Biol.*, vol. 52, no. 10, p. 2637, 2007.
[10] S. K. Davis, B. D. V. Veen, S. C. Hagness, and F. Kelcz, "Breast tumor characterization based on ultrawideband microwave backscatter," *IEEE Trans. Biomed. Eng.*, vol. 55, no. 1, pp. 237–246, Jan. 2008.
[11] M. Jalilvand, X. Li, L. Zwirello, and T. Zwick, "Ultra wideband compact near-field imaging system for breast cancer detection," *IET Microw., Antennas Propag.*, vol. 9, no. 10, pp. 1009–1014, Mar. 2015.
[12] S. M. Aguilar, M. A. Al-Joumayly, M. J. Burfeindt, N. Behdad, and S. C. Hagness, "Multiband miniaturized patch antennas for a compact, shielded microwave breast imaging array," *IEEE Trans. Antennas Propag.*, vol. 62, no. 3, pp. 1221–1231, Mar. 2014.
[13] I. Craddock, M. Klemm, J. Leendertz, A. Preece, and R. Benjamin, "An improved hemispeherical antenna array design for breast imaging," in *Proc. 2nd Eur. Conf. Antennas Propag. (EuCAP)*, 2007, pp. 1–5.
[14] M. M. Islam, M. T. Islam, M. Samsuzzaman, M. R. I. Faruque, N. Misran, and M. F. Mansor, "A miniaturized antenna with negative index metamaterial based on modified SRR and CLS unit cell for UWB microwave imaging applications," *Materials*, vol. 8, no. 2, pp. 392–407, 2015.
[15] J. Zhang, E. C. Fear, and R. H. Johnston, "Cross-Vivaldi antenna for breast tumor detection," *Microw. Opt. Technol. Lett.*, vol. 51, no. 2, pp. 275–280, 2009.
[16] M. M. Islam, M. T. Islam, M. R. I. Faruque, M. Samsuzzaman, N. Misran, and H. Arshad, "Microwave imaging sensor using compact metamaterial UWB antenna with a high correlation factor," *Materials*, vol. 8, no. 8, pp. 4631–4651, 2015.
[17] H. M. Jafari, J. M. Deen, S. Hranilovic, and N. K. Nikolova, "Co-polarised and cross-polarised antenna arrays for breast, cancer detection," *IET Microw., Antennas Propag.*, vol. 1, no. 5, pp. 1055–1058, Oct. 2007.
[18] L. Kurra, M. P. Abegaonkar, A. Basu, and S. K. Koul, "FSS properties of a uniplanar EBG and its application in directivity enhancement of a microstrip antenna," *IEEE Antennas Wireless Propag. Lett.*, vol. 15, pp. 1606–1609, 2016.
[19] R. J. Langley and E. A. Parker, "Double-square frequency-selective surfaces and their equivalent circuit," *Electron. Lett.*, vol. 19, no. 17, pp. 675–677, Aug. 1983.
[20] J. Wang *et al.*, "Broadband planar left-handed metamaterials using split-ring resonator pairs," *Photon. Nanostruct.-Fundam. Appl.*, vol. 7, no. 2, pp. 108–113, 2009.
[21] M. Z. Mahmud, M. T. Islam, N. Misran, M. J. Singh, and K. Mat, "A negative index metamaterial to enhance the performance of miniaturized UWB antenna for microwave imaging applications," *Appl. Sci.*, vol. 7, no. 1, p. 1149, 2017.
[22] G. V. Eleftheriades, A. K. Iyer, and P. C. Kremer, "Planar negative refractive index media using periodically LC loaded transmission lines," *IEEE Trans. Microw. Theory Techn.*, vol. 50, no. 12, pp. 2702–2712, Dec. 2002.
[23] X. Zhou, Y. Liu, and X. Zhao, "Low losses left-handed materials with optimized electric and magnetic resonance," *Appl. Phys. A, Mater. Sci. Process.*, vol. 98, no. 3, pp. 643–649, 2010.
[24] H. Odabasi, F. L. Teixeira, and D. Guney, "Electrically small, complementary electric-field-coupled resonator antennas," *J. Appl. Phys.*, vol. 113, no. 8, p. 084903, 2013.
[25] M. T. Islam, M. M. Islam, M. Samsuzzaman, M. R. I. Faruque, and N. Misran, "A negative index metamaterial-inspired UWB antenna with an integration of complementary SRR and CLS unit cells for microwave imaging sensor applications," *Sensors*, vol. 15, no. 5, pp. 11601–11627, 2015.
[26] M. S. Alam, M. T. Islam, and N. Misran, "A novel compact split ring slotted electromagnetic bandgap structure for microstrip patch antenna performance enhancement," *Prog. Electromagn. Res.*, vol. 130, pp. 389–409, Aug. 2012.
[27] R. Abhari and G. V. Eleftheriades, "Metallo-dielectric electromagnetic bandgap structures for suppression and isolation of the parallel-plate noise in high-speed circuits," *IEEE Trans. Microw. Theory Techn.*, vol. 51, no. 6, pp. 1629–1639, Jun. 2003.

[28] R. C. Hadarig, M. E. de Cos, and F. Las-Heras, "Microstrip patch antenna bandwidth enhancement using AMC/EBG structures," *Int. J. Antennas Propag.*, vol. 2012, 2011, Art. no. 843754.

[29] M. E. de Cos and F. Las-Heras, "Dual-band uniplanar CPW-fed monopole/EBG combination with bandwidth enhancement," *IEEE Antennas Wireless Propag. Lett.*, vol. 11, pp. 365–368, 2012.

[30] M. Mantash, A.-C. Tarot, S. Collardey, and K. Mahdjoubi, "Dual-band CPW-fed G-antenna using an EBG structure," in *Proc. Loughborough Antennas Propag. Conf.*, 2012, pp. 453–456.

[31] M. S. Alam, M. T. Islam, and N. Misran, "Inverse triangular-shape CPW-fed antenna loaded with EBG reflector," *Electron. Lett.*, vol. 49, no. 2, pp. 86–88, Jan. 2013.

[32] N. Wang, H. Tian, Z. Guo, D. Yang, J. Zhou, and Y. Ji, "Bandwidth and gain enhancement of optically transparent 60-GHz CPW-fed antenna by using BSIS-UC-EBG structure," *Photon. Nanostruct.-Fundam. Appl.*, vol. 15, pp. 99–108, Jun. 2015.

[33] M. T. Islam, M. S. Alam, N. Misran, M. Ismail, and B. Yatim, "Development of high gain multiband antenna with centre-offset copper strip-based periodic structure," *Microw. Opt. Technol. Lett.*, vol. 57, no. 7, pp. 1608–1614, 2015.

[34] M. Abbak, M. Çayören, and I. Akduman, "Microwave breast phantom measurements with a cavity-backed Vivaldi antenna," *IET Microw., Antennas Propag.*, vol. 8, no. 13, pp. 1127–1133, Oct. 2014.

[35] C. A. Balanis, *Antenna Theory: Analysis and Design*. Hoboken, NJ, USA: Wiley, 2016.

[36] M. Mahmud, S. Kibria, M. Samsuzzaman, N. Misran, and M. Islam, "A new high performance hibiscus petal pattern monopole antenna for UWB applications," *Appl. Comput. Electromagn. Soc. J.*, vol. 31, no. 4, pp. 373–380, 2016.

[37] N. Ojaroudi, M. Ojaroudi, and Y. Ebazadeh, "UWB/omni-directional microstrip monopole antenna for microwave imaging applications," *Prog. Electromagn. Res. C*, vol. 47, pp. 139–146, Feb. 2014.

[38] K. R. Foster, J. L. Schepps, R. D. Stoy, and H. P. Schwan, "Dielectric properties of brain tissue between 0.01 and 10 GHz," *Phys. Med. Biol.*, vol. 24, no. 6, p. 1177, 1979.

[39] S. Gabriel, R. W. Lau, and C. Gabriel, "The dielectric properties of biological tissues: II. Measurements in the frequency range 10 Hz to 20 GHz," *Phys. Med. Biol.*, vol. 41, no. 11, p. 2251, 1996.

[40] J. Jossinet and M. Schmitt, "A review of parameters for the bioelectrical characterization of breast tissue," *Ann. New York Acad. Sci.*, vol. 873, no. 1, pp. 30–41, 1999.

[41] W. T. Joines, Y. Zhang, C. Li, and R. L. Jirtle, "The measured electrical properties of normal and malignant human tissues from 50 to 900 MHz," *Med. Phys.*, vol. 21, no. 4, pp. 547–550, 1994.

[42] H. B. Lim, N. T. T. Nhung, E.-P. Li, and N. D. Thang, "Confocal microwave imaging for breast cancer detection: Delay-multiply-and-sum image reconstruction algorithm," *IEEE Trans. Biomed. Eng.*, vol. 55, no. 6, pp. 1697–1704, Jun. 2008.

[43] S. Kibria, M. T. Islam, and B. Yatim, "New compact dual-band circularly polarized universal RFID reader antenna using ramped convergence particle swarm optimization," *IEEE Trans. Antennas Propag.*, vol. 62, no. 5, pp. 2795–2801, May 2014.

[44] M. Koutsoupidou *et al.*, "Evaluation of a tumor detection microwave system with a realistic breast phantom," *Microw. Opt. Technol. Lett.*, vol. 59, no. 1, pp. 6–10, 2017.

[45] M. Klemm, I. J. Craddock, J. A. Leendertz, A. Preece, and R. Benjamin, "Radar-based breast cancer detection using a hemispherical antenna array—Experimental results," *IEEE Trans. Antennas Propag.*, vol. 57, no. 6, pp. 1692–1704, Jun. 2009.

[46] M. Klemm, J. A. Leendertz, D. Gibbins, I. J. Craddock, A. Preece, and R. Benjamin, "Microwave radar-based differential breast cancer imaging: Imaging in homogeneous breast phantoms and low contrast scenarios," *IEEE Trans. Antennas Propag.*, vol. 58, no. 7, pp. 2337–2344, Jul. 2010.

[47] D. Zhang and A. Mase, "Experimental study on radar-based breast cancer detection using UWB antennas without background subtraction," *Biomed. Eng., Appl., Basis Commun.*, vol. 23, no. 5, pp. 383–391, 2011.

[48] V. Zhurbenko, T. Rubæk, V. Krozer, and P. Meincke, "Design and realisation of a microwave three-dimensional imaging system with application to breast-cancer detection," *IET Microw., Antennas Propag.*, vol. 4, no. 12, pp. 2200–2211, Dec. 2010.

[49] E. Porter, A. Santorelli, and M. Popovic, "Time-domain microwave radar applied to breast imaging: Measurement reliability in a clinical setting," *Prog. Electromagn. Res.*, vol. 149, pp. 119–132, Sep. 2014.

MD. ZULFIKER MAHMUD received the B.Sc. and M.Sc. degrees in computer science and engineering from Islamic University Kushtia, Bangladesh, and the Ph.D. degree from the Universiti Kebangsaan Malaysia (UKM), Malaysia. He was a Graduate Research Assistant with the Department of Electrical, Electronic and Systems Engineering, UKM, Malaysia. He is currently an Assistant Professor with the Department of AIS, Jagannath University, Bangladesh. He has authored or co-authored a number referred journals and conference papers. His research interests include microwave imaging, antenna design, satellite antennas, satellite communication, and wireless communication.

MOHAMMAD TARIQUL ISLAM is currently a Professor with the Department of Electrical, Electronic and Systems Engineering, Universiti Kebangsaan Malaysia (UKM). He is also the Group Leader of the Radio Astronomy Informatics Group, UKM. He has authored over 300 research journal articles, nearly 165 conference articles, and a few book chapters on various topics related to antennas, microwaves, and electromagnetic radiation analysis with 11 inventory patents filed. Thus far, his publications have been cited 1990 times and his H-index is 25 (Source: Scopus). He is currently handling many research projects from the Malaysian Ministry of Science, Technology and Innovation, the Ministry of Education, and some international research grants from Japan. His research interests include communication antenna design, radio astronomy antennas, satellite antennas, and electromagnetic radiation analysis.

NORBAHIAH MISRAN received the B.Eng. degree in electrical, electronic and system engineering from the Universiti Kebangsaan Malaysia (UKM) in 1999, and the Ph.D. degree from the Queen's University of Belfast, Northern Ireland, U.K., in 2004. She started her career as a Tutor in 1999. She later has been appointed as a Lecturer in 2004 and an Associate Professor in 2009. She is currently a Professor at UKM. Her research interests include RF device design particularly in broadband microstrip antennas, reconfigurable antennas, and reflect array antennas. She is also conducting some researches in engineering education field.

SALEHIN KIBRIA was born in Dhaka, Bangladesh, in 1988. He received the B.Eng. degree (Hons.) in electronics majoring in telecommunications from Multimedia University, Malaysia. He is currently pursuing the Ph.D. degree with the Universiti Kebangsaan Malaysia. He is also a Research Assistant at the Institute of Space Science (ANGKASA) in a research project funded by the Malaysian government. His research interest focuses on RFID reader antenna designs, telecommunication, and particle swarm optimization.

MD. SAMSUZZAMAN was born in Jhenaidah, Bangladesh, in 1982. He received the B.Sc. and M.Sc. degrees in computer science and engineering from the Islamic University Kushtia, Bangladesh, in 2005 and 2007, respectively, and the Ph.D. degree from the Universiti Kebangsaan Malaysia, Malaysia, in 2015. From 2008 to 2011, he was a Lecturer with the Patuakhali Science and Technology University, Bangladesh, where he was an Assistant Professor from 2011 to 2015. He was an Associate Professor with the Patuakhali Science and Technology University. He is currently a Post-Doctoral Fellow with Universiti Kebangsaan Malaysia. He has authored or co-authored approximately 50 referred journals and conference papers. His research interests include the communication antenna design, satellite antennas, and satellite communication.